Chinese Chemical Letters 34 (2023) 107737

Contents lists available at ScienceDirect

Chinese Chemical Letters

journal homepage: www.elsevier.com/locate/cclet

Abietane derived diterpenoids as $Ca_v3.1$ antagonists from *Salvia digitaloides*

Jianjun Zhao[a,c,1], Shuzong Du[b,c,1], Kun Hu[a,1], Yali Hu[a,c], Fan Xia[a], Yansong Ye[a], Jian Yang[d], Yin Nian[a,*], Gang Xu[a,*]

[a] State Key Laboratory of Phytochemistry and Plant Resources in West China, Kunming Institute of Botany, Chinese Academy of Sciences, and Yunnan Key Laboratory of Natural Medicinal Chemistry, Kunming 650201, China
[b] Key Laboratory of Animal Models and Human Disease Mechanisms, and Ion Channel Research and Drug Development Center, Kunming Institute of Zoology, Chinese Academy of Sciences, Kunming 650223, China
[c] University of Chinese Academy of Sciences, Beijing 100049, China
[d] Department of Biological Sciences, Columbia University, New York, NY 10027, United States

ARTICLE INFO

Article history:
Received 25 May 2022
Revised 30 July 2022
Accepted 8 August 2022
Available online 10 August 2022

Keywords:
10-Methylated 6/7/6 carbon ring system
Icetexane
Diterpenoid
Salvia digitaloides
$Ca_v3.1$ low voltage-gated Ca^{2+} channel (LVGCC)

ABSTRACT

Nineteen diterpenoids, including saldigitin A (**1**) bearing an unprecedented 10-methylated 6/7/6 carbon ring system, two new icetexanes (**2**, **3**), and two new *nor*-abietanes (**5**, **6**) were characterized from the roots of *Salvia digitaloides*. Their structures were elucidated by the analysis of the spectroscopic data, X-ray crystallography, and TDDFT calculations of ECD spectra. The novel architecture of **1** should be biogenetically derived through the cleavage and re-cyclization of the B/C rings from the normal abietane skeleton. Biologically, **1**–**5** exhibited noticeable inhibitions on $Ca_v3.1$ low voltage-gated Ca^{2+} channel (LVGCC), with IC_{50} values in the range of 3.43–11.70 μmol/L. They are the first example of diterpenoids with 6/7/6 carbon rings system as $Ca_v3.1$ antagonists.

Salvia, one of the largest genera in the economically and medicinally important family Lamiaceae, is distributed worldwide and arises the folkloric belief of its "magical" therapeutic properties for various indispositions [1]. Investigations on *Salvia* plants have led to the discovery of a number of secondary metabolites, mainly diterpenoids and polyphenols [1–5]. Of these, abietanes and clerodanes have been identified as typical metabolites with diverse structures and significant bioactivities, such as salvicine (a significant antitumor agent), tanshinone IIA (a cardioprotective agent), salvinorin A (a potent agonist at the κ-opioid receptor), and *neo*-tanshinlactone (a significant and selective inhibitor against two ER human breast cancer cells) [1–5].

Our group has been investigating the diterpenoid constituents of *Salvia* since 2000, and has discovered many diterpenoids with attractive bioactivities [6–12]. *Salvia digitaloides* is an indispensable ingredient of a special traditional "red wine" by local Tibetans to strengthen their physical health [13]. Previously, twelve iridoids, four isoprenylated flavonoids, and fifteen abietane diterpenoids have been discovered from its roots [14–17]. Recently, several diterpenoids such as salpratlactones A and B, a pair of *cis-trans* tautomeric abietanes isolated from *S. prattii*, have been identified as the first $Ca_v3.1$ agonists [10]. In order to explore more diterpenoids with bioactivities on $Ca_v3.1$, the roots of *S. digitaloides* were phytochemically investigated in this study.

In our continuous investigation on *S. digitaloides*, another nineteen diterpenoids including five new ones, saldigitins A–E (**1**–**3**, **5**, and **6**) were isolated and identified (Fig. 1). Notably, saldigitin A (1) was elucidated to possess an unprecedented 10-methylated 6/7/6 carbon ring system. And the skeleton of **1** should be biogenetically derived through cleavage and re-cyclization of the B/C rings of normal abietane skeleton, which was distinct from the biopathway for icetexane type diterpenoids with a methyl-20-incorporated 6/7/6 carbon scaffold such as compounds **2**–**4** in this study. The structures of isolated compounds were assigned by extensive analysis of their spectroscopic data, and the absolute configuration of **1**–**3**, and **5** were determined either by X-ray crystallography or theoretical calculations of their electronic circular dichroism (ECD) spectra. In addition, we initially disclosed that **1**–**5** notably inhibited the peak currents of $Ca_v3.1$ low voltage-gated Ca^{2+} channel (LVGCC), an attractive therapeutic target for neuropathic pain, absence epilepsy,

* Corresponding authors.
E-mail addresses: nianyin@mail.kib.ac.cn (Y. Nian), xugang008@mail.kib.ac.cn (G. Xu).
[1] These authors contributed equally to this work.

https://doi.org/10.1016/j.cclet.2022.08.017
1001-8417/

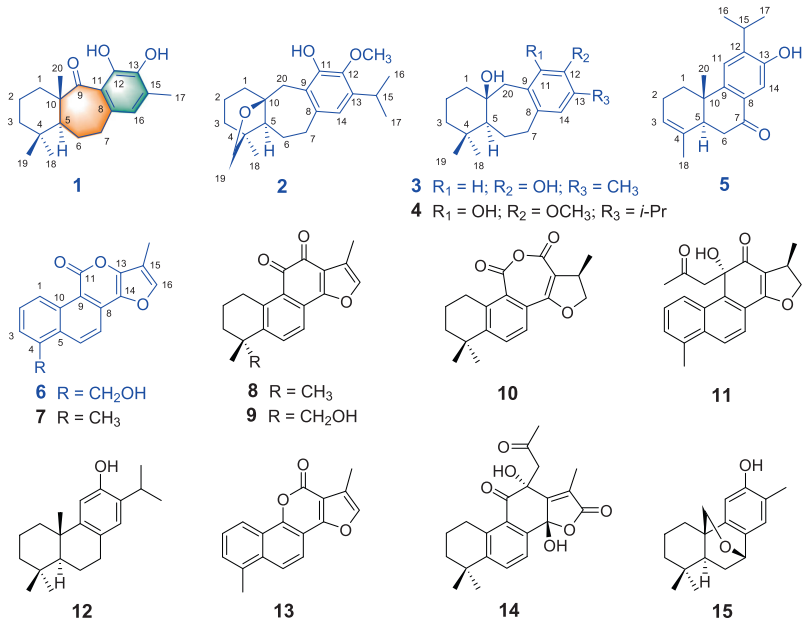

Fig. 1. Structures of **1**–**15**.

insomnia, and Parkinson's tremors [18–20], in a dose-dependent manner with IC_{50} values of 7.08, 10.09, 11.70, 4.97, and 3.43 μmol/L, respectively. In addition, it is the first report of icetexane and related diterpenoids possessing 6/7/6 carbon rings system with antagonistic activities on $Ca_V3.1$. Reported herein are the isolation, structure characterization, proposed biogenetic pathways, and biological evaluation of these compounds.

Saldigitin A (**1**) was isolated as a colorless needle crystal and its molecular formula was determined as $C_{19}H_{26}O_3$ by HRESIMS (*m/z* 301.1814 $[M - H]^-$, calcd. for $C_{19}H_{25}O_3$, 301.1809), including 7 degrees of unsaturation. The IR spectrum displayed bands for hydroxy (3472 cm^{-1}) and carbonyl (1614 cm^{-1}) groups. Besides, the ^{13}C NMR spectrum presented 19 carbon signals ascribed to eight quaternary carbons (including one ketone and five olefinic), two methines (including an olefinic one), five methylenes, and four methyls. The three double bonds and one keto moiety accounted for four degrees of unsaturation, suggesting the tricyclic skeleton of **1**. In addition, the characteristic signals for abietane type diterpenoid including three singlet methyls [δ_H 0.84, δ_C 33.2, Me-18; δ_H 0.93, δ_C 23.1, Me-19; and δ_H 1.28, δ_C 16.9, Me-20], five typical methylenes [δ_H 1.94 (m), 1.23 (m), δ_C 40.0, H_2-1; δ_H 1.63 (m), 1.47 (m), δ_C 18.9, H_2-2; δ_H 1.32 (m), 1.09 (m), δ_C 42.6, H_2-3; δ_H 1.95 (m), 1.79 (m), δ_C 25.1, H_2-6; δ_H 2.64 (m), 2.56 (m), δ_C 31.0, H_2-7], and two aliphatic quaternary carbons [δ_C 34.3, C-4; δ_C 50.8, C-10] indicated that **1** should be an abietane derivative [1–12].

Normally, the chemical shifts of C-10 and Me-20 for an abietane diterpenoid were presented at δ_C 36–43 (s) and δ_C 22–28 (q), respectively, in the ^{13}C NMR spectrum [21,22]. Whereas in **1**, these two characteristic signals were replaced by two distinct signals at δ_C 50.8 (s) and 16.9 (q), respectively (Table 1). In addition, a carbonyl group at δ_C 219.0 (C-9) and the typical methylene (CH_2-1) were presented simultaneously. These observations showed that the structure of **1** was quite different from those of common abietanes with ordinary 6/6/6-membered ring system.

The HMBC correlations of Me-20 with C-9, and the mentioned carbonyl carbon at δ_C 219.0 led to the assignment of the ketone carbonyl group at C-9. The connection of C-5/C-6/C-7 was accomplished by the proton spin system of H-5/H_2-6/H_2-7 observed in the ^1H-^1H COSY spectrum. Furthermore, the HMBC correlations of

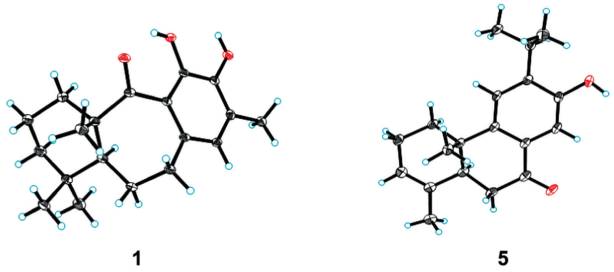

Fig. 2. X-ray crystal structures of **1** and **5**.

H-5 with C-7, C-9, and C-10, H-7 and H-16 with C-8, C-9 and C-11 further established the linkage of C-5/C-10 (Me-20)/C-9/C-11/C-8/C-7, which evidently showed the unprecedented 10-methylated seven-membered ring B. The six-membered ring A was established by the HMBC associations of the geminal Me-18 and Me-19 with C-3, C-4, and C-5, of Me-20 with C-1, C-5, and C-10, conjugated with the proton spin system H_2-1/H_2-2/H_2-3 (Fig. S1 in Supporting information). Similarly, the HMBC couplings from the singlet Me-17 (δ_H 2.22) to C-13, C-15, and C-16, from the unsaturated methine signal at δ_H 6.40 (1H, s, H-16) to C-11, C-13, C-17, C-8, and C-15, confirmed the existence of aromatic C ring. Thus, the 2D structure of **1** was established.

Assigning H-5 as α-oriented, the large coupling constant ($^3J_{H\text{-}5/H\text{-}6b} = 12.2$ Hz) indicated that H-6b (δ_H 1.79, m) adopted β-orientation [23]. The correlations of H_3-18/H-5α, H_3-19/H-6β, and H_3-20/H_3-19 observed in the ROESY spectrum revealed that Me-20 was β-oriented. Finally, a fine single crystal of **1** was obtained and the X-ray crystallographic data [Flack parameter = 0.01(6), CCDC: 2120506] further confirmed its absolute configuration as 5*S*, 10*S* (Fig. 2).

Biogenetically, compound **1** might rationally be generated from a common abietane precursor ferruginol (**12**) undergoing epoxidation to form 9,11-epoxide **i** [24]. A pinacol rearrangement occurs from **i** with acidic conditions lead to a B-homo-C-nor-abietane with a rearranged 6/7/5 ring system (**ii**) [11]. Meanwhile, the C-13/C-14 double bond further be oxidized to form two ketones (C-

Table 1
^{1}H (600 MHz) and ^{13}C (150 MHz) NMR spectroscopic data for compounds **1**–**3**, **5**, and **6**.

No.	**1**[a]		**2**[a]		**3**[b]		**5**[a]		**6**[b]	
	δ_C	δ_H (J in Hz)	δ_C	δ_H (J in Hz)	δ_C	δ_H (J in Hz)	δ_C	δ_H (J in Hz)	δ_C	δ_H (J in Hz)
1a	40.0	1.94, m (α)	40.1	1.74, dd (12.7, 5.7)	41.9	1.39, m (β)	32.6	2.52, dd (18.0, 14.0)	120.8	8.35, d (8.2)
1b		1.23, m (β)		1.54, dd (12.7, 5.7)		1.61, m (α)		1.65, m		
2a	18.9	1.63, m (β)	20.5	1.88, m	18.3	1.30, m (α)	22.9	2.21, m	127.3	7.70, dd (7.1, 8.1)
2b		1.47, m (α)		1.59, m		1.73, m (β)				
3a	42.6	1.32, m	39.7	1.40, m	42.3	1.16, m	122.4	5.47, s	126.6	7.75, d (7.1)
3b		1.09, m								
4	34.3		44.2		34.0		132.9		138.7	
5	46.1	1.55, dd (12.2, 5.0)	54.8	1.48, m	57.0	1.16, m	44.2	2.77, br d (14.6)	131.5	
6a	25.1	1.95, m	24.1	1.88, m	23.1	1.72, m	38.1	2.86, d (4.3)	121.0	8.08, d (8.7)
6b		1.79, m		1.40, m		1.35, m		2.83, d (4.3)		
7a	31.0	2.64, m (β)	32.3	2.76, m	34.8	2.50, m (β)	199.7		117.0	7.96, d (8.7)
7b		2.56, m (α)		2.81, m		2.60, m (α)				
8	130.2		139.6		136.1		130.1		107.7	
9	219.0		121.4		133.0		147.0		148.8	
10	50.8		84.9		70.1		36.0		122.7	
11	121.7		146.9		118.0	6.46, s	121.9	7.23, s	157.6	
12	143.9		142.5		152.7		142.5			
13	141.5		138.7		120.2		152.2		109.9	
14			116.9	6.47, s	130.1	6.70, s	113.6	7.60, s	157.9	
15	128.6		26.6	3.18, sept (6.9)	15.5	2.03, s	28.1	3.32, sept (7.0)	119.4	
16	121.6	6.40, s	24.1	1.20, d (6.9)			22.5	1.25, d (7.0)	142.8	7.98, q (1.6)
17	16.0	2.22, s	24.0	1.19, d (6.9)			22.5	1.24, d (7.0)	8.3	2.31, d (1.0)
18	33.2	0.84, s	19.3	0.87, s	32.3	0.85, s	21.1	1.66, s	61.2	5.00, d (5.1)
19	23.1	0.93, s	77.1	3.71, d (7.9)	21.8	0.83, s				
				3.57, d (7.9)						
20a	16.9	1.28, s	34.3	3.08, d (14.3)	51.1	2.76, d (14.0) (α)	21.9	1.10, s		
20b				2.97, d (14.3)		2.31, d (14.0) (β)				
OMe			62.0	3.73, s (MeO-12)						
OH				5.64, s (HO-11)		3.12, s (HO-10); 8.72, s (HO-12)		6.46, s (HO-13)		

[a] Recorded in chloroform-*d*.
[b] Recorded in DMSO-d_6.

13 and C-14). Subsequently, decarboxylation of C-14 proceeded to form a carbanion (C-8), which attached the terminal olefinic link (CH_2-16) *via* a Michael reaction to build up the six-membered ring C (**iii**), and then undergoes oxidation reaction to form the structure of **1** [10,25,26]. Biogenetically, icetexane diterpenoids, with a similar 6/7/6 skeleton, were believed to arise from a rearrangement of normal abietane and chemically belong to the 9(10→20) abeo-abietane framework with a 6/7/6-membered ring system [1,27,28]. Accordingly, **1** possesses a unique methyl at C-10 that derived from a distinct way of the cleavage of both rings B and C, and then re-cyclization to form the unprecedented 6/7/6 ring system which should be distinct from that for the normal icetexane (Scheme 1).

Saldigitin B (**2**) was obtained as a white powder, and gave rise to a $[M+H]^+$ peak at m/z 331.1165 (calcd. 331.2268) in the positive-ion-mode HRESIMS, corresponding to the molecular formula $C_{21}H_{30}O_3$. Detailed analysis of its 1D NMR data revealed that the signals for the characteristic aliphatic quaternary carbon [C-10 (δ_C 36–43)] and the methyl group [Me-20 (δ_C 22–28)] of normal abietanes were absent in **2** [25,26]. Besides, the observation that H-20a and H-20b appeared as an AB system at δ_H 3.08, 2.97 (1H each d, $J=14.3$ Hz) further confirmed that **2** is an icetexane-type compound with a typical seven-membered ring B [25,26]. Structurally, **2** is quite similar to salvicanol (**4**) except for the replacement of a methyl with an oxygenated methylene in **2** [29,30]. The long-range HMBC correlations (Fig. S2 in Supporting information) from H_2-19 (δ_H 3.71, 3.57, d, $J=7.9$ Hz) to C-3, C-4 (δ_C 44.2), C-5 (δ_C 54.8), C-10 (δ_C 84.9), and C-18 (δ_C 19.3), and from H_2-1 (δ_H 1.74, 1.54, dd, $J=12.7$, 5.7 Hz) to C-5, C-10, and C-20 (δ_C 34.3) confirmed the presence of an ether bridge between C-10 and C-19. For biogenetic reasons, H-5 and Me-18 were expected to be cofacial and adopt an α-orientation as established by the ROESY correlations of H-7α/H-5/H_3-18/H-2α. To determine the absolute configuration of saldigitin B (**2**), (4*S*,5*S*,10*S*)-**2** was subjected to TDDFT ECD calculations at two independent levels of theory: CAM-B3LYP-SCRF/6-311+G(2d,p) (methanol, IEFPCM solvent model) and PBE0-SCRF/6-311+G(2d,p) (methanol, IEFPCM solvent model). At both levels of theory, the calculated ECD spectra matched well with their experimental counterpart (Fig. S4 in Supporting information). Consequently, the structure of saldigitin B (**2**) was assigned and its absolute configuration was determined as 4*S*, 5*S*, and 10*S*.

Saldigitin C (**3**), isolated as a white amorphous powder, and showed a molecular ion at m/z 273.1866 $[M-H]^-$ in the HRESIMS (calcd. 273.1860), which correlated to the molecular formula $C_{18}H_{26}O_2$. Comparison of its 1D NMR spectroscopic data (Table 1) with those of pisiferanol indicated they were similar to each other except that the isopropyl group at C-13 in pisiferanol was replaced by a methyl group in **3** [28]. This deduction was confirmed by the HMBC correlations from Me-15 (δ_H 2.03, s) to C-12 (δ_C 152.7), C-13 (δ_C 120.2), and C-14 (δ_C 130.1) [28]. As in the case of **2**, Me-19 of icetexane diterpenoid was expected to be β-oriented, while H-5 and Me-18 were α-oriented. Furthermore, the ROESY cross-peaks of HO-10/H_3-19, H-1a, H-2b, H-20b, and H-7a confirmed that they were spatially close and can be assigned as β-oriented. Consequently, the correlations of H-5/H_3-18, H-7b, H-20a, and H-1b indicated that they were cofacial and adopt an α-orientation. The absolute configuration of saldigitin C (**3**) was also established by TDDFT ECD calculations. At both levels of theory, the calculated ECD spectra of (5*S*,10*S*)-**3** were found to be consistent with the experimental spectrum (Fig. S4). Accordingly, the absolute configuration of **3** was determined as 5*S* and 10*S*.

Saldigitin D (**5**) was isolated as a white needle crystal and was assigned the molecular formula $C_{19}H_{24}O_2$, based on HRESIMS (m/z 285.1844 $[M+H]^+$, calcd. $C_{19}H_{25}O_2$, 285.1849). Analysis of its 1D and 2D NMR data revealed that **5** possessed similar scaffold to that

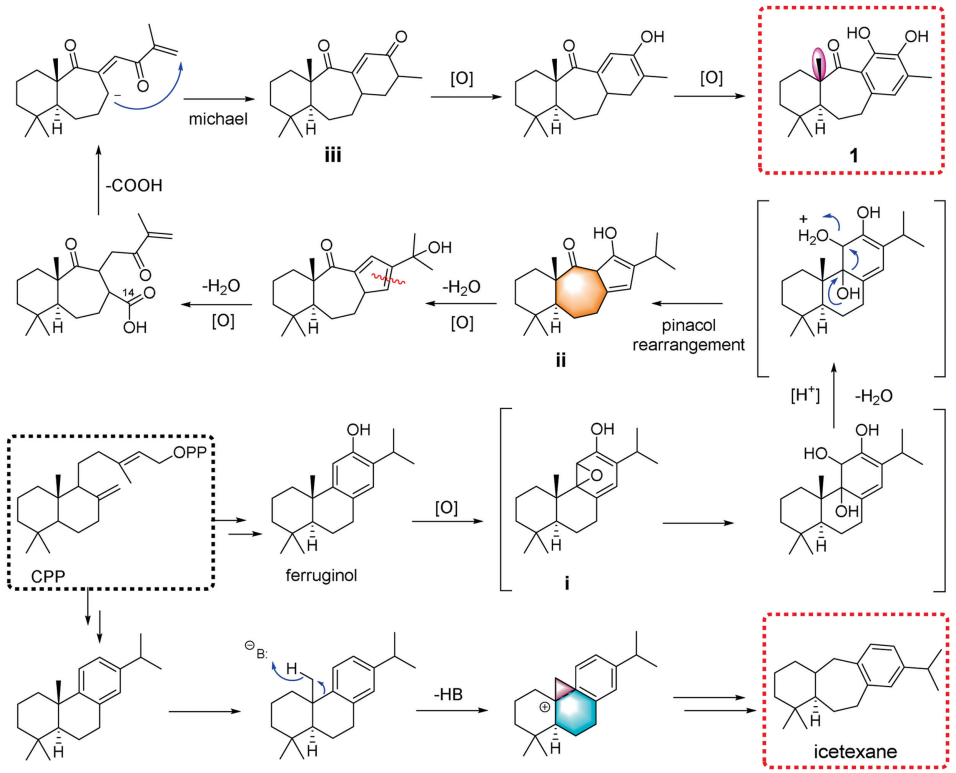

Scheme 1. Putative biosynthetic pathway to **1**.

of 7-keto-sempervirol (**18**) [31–33]. Their key difference was the presence of a trisubstituted olefin at the C-3 and C-4 in **5** instead of the saturated single bond in 7-keto-sempervirol. This elucidation was confirmed by the HMBC correlations from Me-18 (δ_H 1.66, s) to C-3, C-4, and C-5, from H-5 (δ_H 2.77, br d, J = 14.6 Hz) to C-3, C-4, and C-18, and the ^{1}H-^{1}H COSY spin system H_2-1/H_2-2/H-3. In addition, the location of the isopropyl moiety at C-12 was supported by the HMBC correlations from Me-16 and Me-17 to C-12. Furthermore, a single-crystal X-ray analysis (CCDC: 2120507) successfully confirmed the established structure (Fig. 2 and Fig. S3 in Supporting information), however, the Flack parameter (–0.35(8)) was insufficient to unambiguously determine its absolute configuration. Then, TDDFT ECD calculations were run on (5*S*,10*S*)-**5** and revealed the absolute configuration of **5** to be 5*S* and 10*S* (Fig. S4). So, the structure of **5** was established and named saldigitin D.

Saldigitin E (**6**) was obtained as a pink powder. Its molecular formula was established as $C_{17}H_{12}O_4$ by ^{13}C NMR and HRESIMS (*m*/*z* 281.0812 $[M+H]^+$, calcd. $C_{17}H_{13}O_4$, 281.0808). The 1D NMR data of **6** were similar to those of tanshinlactone (**7**) except for the presence of an additional hydroxymethyl group at δ_H 5.00 (d, J = 5.1 Hz, H_2-18) in **6** instead of the Me-18 in tanshinlactone (**7**) [34]. This deduction was supported by HMBC correlations from H_2-18 to C-3 (δ_C 126.6), C-4 (δ_C 138.7), and C-5 (δ_C 131.5), from H-3 (δ_H 7.75, d, J = 7.1 Hz) to C-18 (δ_C 61.2) (Fig. S3). Thus, **6** was assigned as 18-hydroxy-tanshinelactone and named saldigitin E.

In addition, salvicanol (**4**) [29,30], tanshinlactone (**7**) [34], tanshinone IIA (**8**) [24], tanshinone IIB (**9**) [35], cryptotanshinone anhydride (**10**) [36], danshenol A (**11**) [37], ferruginol (**12**) [24], *neo*-tanshinlactone (**13**) [38], salviprzol A (**14**) [39], przewalskin (**15**) [36], 15,16-dihydrotanshinone I (**16**) [24], 16,17-dinorpisferal A (**17**) [14], 7-keto-sempervirol (**18**) [31], and15-*epi*-danshenol A (**19**) [40], were carefully identified by comparison of their spectroscopic data with literature values, and their putative biogenetic relationships are shown in Scheme S1 (Supporting information).

As stated in the introduction, agents with $Ca_v3.1$ LVGCC regulatory effects may have promising potential to treat several neurological disorders [18–20]. In the present study, we firstly revealed that four new compounds, saldigitins A–D (**1**–**3**, and **5**), as well as the known one, salvicanol (**4**), dose-relatedly blocked $Ca_v3.1$ peak currents among their testing concentration range (Fig. 3 and Table S1 in Supporting information). The IC_{50} values of **1**–**5** on $Ca_v3.1$ are 7.08, 10.09, 11.70, 4.97, and 3.43 μmol/L, respectively. Mibefradil, the positive control, showed stronger activity than **1**–**5**, with an IC_{50} value of 1.12 μmol/L (Fig. S12 in Supporting information). As shown in Fig. 3, compared to **2**, **4**, and **5**, the blockages of **1** and **3** were more difficult to wash out, suggesting these two ones may have deeper binding sites inside the channel. Saldigitin E (**6**) showed negligible effect on $Ca_v3.1$ at the concentration of 10 μmol/L (Fig. S11 in Supporting information). The structure–function relationships and action characteristics of those active compounds deserve to be elucidated in future.

To the best of our knowledge, compound **1** can be seen as the first diterpenoid featuring an unprecedented 10-methylated 6/7/6 carbon ring system. In comparison with normal icetexanes with a 10-unmethylated 6/7/6 carbon scaffold, **1** should be derived from a distinct biopathway from the normal abietane skeleton undergone the cleavage of rings B/C and then re-cyclization. The 6/7/6-tricyclic core structure of icetexanes were also constructed *via* natural rearrangement of more normal 6/6/6-fused abietane diterpenoids [1]. These diterpenoids have aroused great attentions from the synthetic communities for their interesting structures as well as significant bioactivities [41–46]. In the bioactive assay, we firstly revealed that four diterpenoids with 6/7/6 carbon skeleton, **1**–**4**, and a 19-*nor*-15(13→12)-abeo-abietane (**5**) showed notable inhibitory effects on $Ca_v3.1$ LVGCC, which may have promising potential to treat several neurological disorders. In summary, about 70 icetexanes with the normal 6/7/6 skeleton have been identified and synthesized so far [8,41–44], the present study provides new

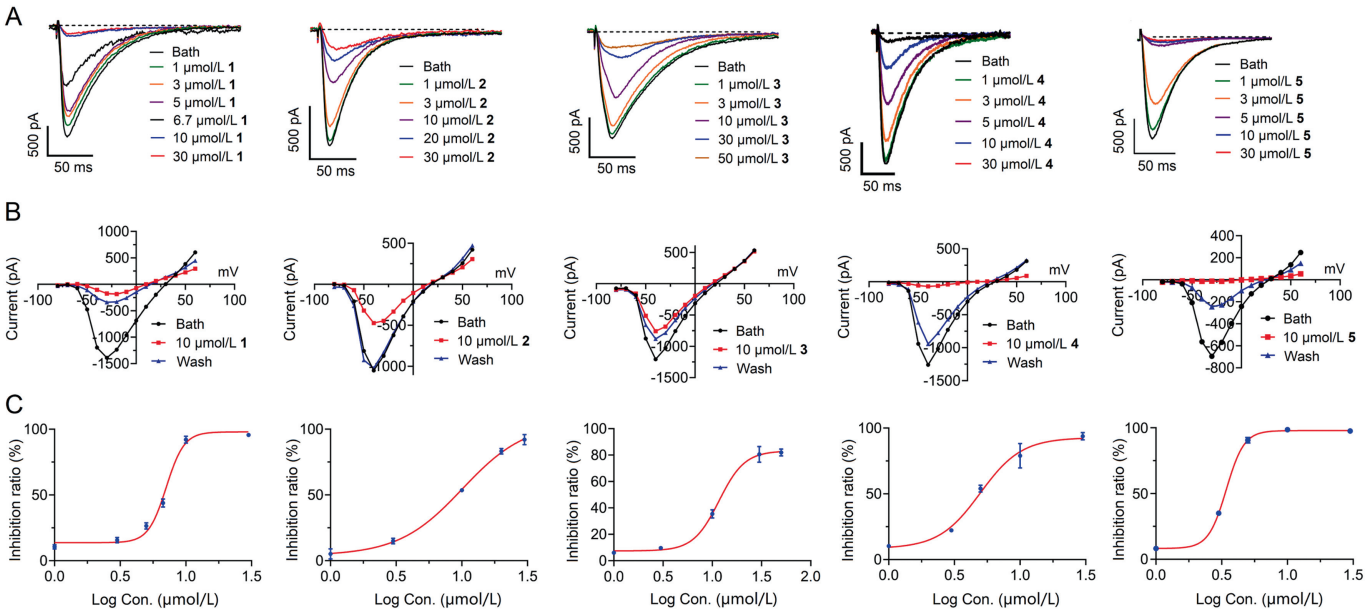

Fig. 3. Inhibitory effect of compounds **1**–**5** on $Ca_v3.1$. (A) Representative $Ca_v3.1$ peak current traces elicited by 150 ms depolarization to −30 mV at 4 s intervals from a holding potential (HP) of −100 mV in the absence (control) and presence of different concentrations of **1**–**5**, respectively. (B) Current-voltage (*I-V*) curves of $Ca_v3.1$ in the absence or presence of **1**–**5** at 10 μmol/L. $Ca_v3.1$ currents were evoked from a holding HP of −100 mV by 150 ms depolarization from −80 mV to +60 mV in 10 mV increasement at 4 s intervals. (C) Dose-response relationships of **1**–**5** for $Ca_v3.1$ at HP of −100 mV, respectively. Data points represent mean ± SD of three to five measurements. The solid curve represents a fit to the Hill equation. The IC_{50} values of **1**–**5** are 7.08, 10.09, 11.70, 4.97, and 3.43 μmol/L, respectively.

perspectives for the structures and biological activities of the diterpenoids with 6/7/6 carbon ring system.

Declaration of competing interest

The authors declare that they have no known competing financial interests or personal relationships that could have appeared to influence the work reported in this paper.

Acknowledgments

This work was financially supported by the National Natural Science Foundation of China (Nos. 32070392 and 32070393), the Second Tibetan Plateau Scientific Expedition and Research (STEP) Program (Nos. 2019QZKK0502-0303 and 2019QZKK0502-0304), Natural Science Foundation of Yunnan Province (Nos. 202001AS070040 and 202101AV070010), Yunnan Young & Elite Talents Project (No. YNWR-QNBJ-2020-277), and CAS "Light of West China" Program (2021).

Supplementary materials

Supplementary material associated with this article can be found, in the online version, at doi:10.1016/j.cclet.2022.08.017.

References

[1] Y.B. Wu, Z.Y. Ni, Q.W. Shi, et al., Chem. Rev. 112 (2012) 5967–6026.
[2] Y.B. Dong, S.L. Morris-Natschke, K.H. Lee, Nat. Prod. Rep. 28 (2011) 529–542.
[3] M. Xue, Y.B. Shi, Y. Chui, et al., Nat. Prod. Res. Dev. 12 (2000) 27–32.
[4] T.A. Munro, M.A. Rizzacasa, B.L. Roth, et al., J. Med. Chem. 48 (2005) 345–348.
[5] M. Xiao, L. Wei, L. Li, et al., Org. Chem. 79 (2014) 2746–2750.
[6] G. Xu, A.J. Hou, R.R. Wang, et al., Org. Lett. 8 (2006) 4453–4456.
[7] G. Xu, A.J. Hou, Y.T. Zheng, et al., Org. Lett. 9 (2007) 291–293.
[8] G. Xu, X.W. Yang, C.Y. Wu, et al., Chem. Commun. 48 (2012) 4438–4440.
[9] C.Y. Wu, Y. Liao, Z.G. Yang, et al., Phytochemistry 106 (2014) 171–177.
[10] F. Xia, W.Y. Li, X.W. Yang, et al., Org. Lett. 21 (2019) 5670–5674.
[11] F. Xia, D.W. Zhang, C.Y. Wu, et al., Org. Chem. Front. 5 (2018) 1262.
[12] G. Xu, L.Y. Peng, L. Lu, et al., Planta Med. 72 (2006) 84–86.
[13] Kunming Institute of Botany, Chinese Academy of Sciences, Flora Yunnannica, Science Press, Beijing, 1977, p. 661.
[14] G. Xu, J. Yang, Y.Y. Wang, et al., J. Agric. Food Chem. 58 (2010) 12157–12161.
[15] S.J. Wu, H.H. Chan, T.L. Hwang, et al., Tetrahedron Lett. 51 (2010) 4287–4290.
[16] S.J. Wu, Y.Y. Chan, Molecules 19 (2014) 15521–15534.
[17] J.J. Zhao, S.Y. Li, F. Xia, et al., Nat. Prod. Bioprospect. 11 (2021) 671–678.
[18] G.W. Zamponi, Nat Rev Drug Discov. 15 (2016) 19–34.
[19] E.J. Cheong, H.S. Shin, Physiol. Rev. 93 (2013) 961–992.
[20] K.H. Choi, Expert Opin. Drug Dis. 8 (2013) 919–931.
[21] A. Ulubelen, S. Öksüz, G. Topcu, et al., J. Nat. Prod. 64 (2001) 549–551.
[22] M. Tada, T. Hara, C. Hara, et al., Phytochemistry 45 (1997) 1474–1477.
[23] Y.Y. Fan, L.S. Gan, H.C. Liu, et al., Org. Lett. 19 (2017) 4580 –4580.
[24] S.Y. Lee, D.Y. Choi, E.R. Woo, Arch. Pharm. Res. 28 (2005) 909–913.
[25] T.D.H. Bugg, Tetrahedron 59 (2003) 7075–7101.
[26] O. Hayaishi, M. Katagiri, S. Rothberg, J. Am. Chem. Soc. 77 (1955) 5450–5451.
[27] E.M. Simmons, J.R. Yen, R. Sarpong, Org. Lett. 14 (2007) 2705–2708.
[28] G. Xu, L.Y. Peng, Y. Zhao, et al., Chem. Pharm. Bull. 53 (2005) 1575–1576.
[29] B.M. Fraga, A.G. Gonzalez, J.R. Herrera, et al., Phytochemistry 25 (1985) 269–271.
[30] M. Bruno, G. Savona, F. Piozzi, et al., Phytochemistry 30 (1991) 2339–2343.
[31] L. Mangoni, R. Caputo, Tetrahedron Lett. 8 (1967) 673–675.
[32] C. Bustos-Brito, P. Joseph-Nathan, E. Burgueño-Tapia, et al., J. Nat. Prod. 82 (2019) 1207–1216.
[33] N.M. Tam, L.T. Hieu, N.M. Thong, et al., Chem. Phys. Lett. 777 (2021) 138737.
[34] H.W. Luo, J. Ji, M.Y. Wu, et al., Chem. Pharm. Bull. 34 (1986) 3166–3168.
[35] X.Y. Yu, S.G. Lin, Z.W. Zhou, et al., Neurosci. Lett. 417 (2007) 261–265.
[36] B. Li, F.D. Niu, Z.W. Lin, et al., Phytochemistry 30 (1991) 3815–3817.
[37] G. Nagy, G. Gunther, I. Mathe, et al., Biochem. Syst. Ecol. 26 (1998) 797–799.
[38] X.H. Wang, K.F. Bastow, C.M. Sun, et al., J. Med. Chem. 47 (2004) 5816–5819.
[39] Y.B. Xue, Y. Wu, H.C. Zhu, et al., Fitoterapia 99 (2014) 204–210.
[40] R. Kasimu, P. Basnet, Y. Tezuka, et al., Chem. Pharm. Bull. 45 (1997) 564–566.
[41] W. Cao, T.T. Liu, S.T. Yang, et al., J. Nat. Prod. 84 (2021) 2012–2019.
[42] A. Hymavathi, K. Suresh Babu, V.G.M. Naidu, et al., Bioog. Med. Chem. Lett. 19 (2009) 5727–5731.
[43] G.J. Zheng, A.K. Kadir, X.F. Zheng, et al., Org. Chem. Front. 7 (2020) 3137–3145.
[44] D.L. Chem, X.Y. Liu, H. Cheng, et al., Chin. Chem. Lett. 22 (2011) 774–776.
[45] Q.T. Le, L.H. Guo, S.L. Lee, et al., Org. Lett. 22 (2020) 9225–9228.
[46] J. Zhang, Y.H. Jin, F.Y.G. Qiu, Org. Lett. 22 (2020) 7415–7418.